Hindawi
Mathematical Problems in Engineering
Volume 2018, Article ID 4539054, 9 pages
https://doi.org/10.1155/2018/4539054

Research Article

Transient Thermal-Electric Simulation and Experiment of Heat Transfer in Welding Tip for Reflow Soldering Process

Jatuporn Thongsri

Computer Simulation in Engineering Research Group, College of Advanced Manufacturing Innovation, King Mongkut's Institute of Technology Ladkrabang, Bangkok, 10520, Thailand

Correspondence should be addressed to Jatuporn Thongsri; jatuporn.th@kmitl.ac.th

Received 7 October 2018; Accepted 3 December 2018; Published 20 December 2018

Guest Editor: Anders E. W. Jarfors

Welding tip is an appliance for making footprint to connect the arm and head gimbal assembly (HGA) together in reflow soldering process. The welding tip is made from 3 materials: copper alloy, stainless steel, and haynes 230. It works based on Joule heating effect. The haynes 230 head tip is the area used to create a footprint. In the past, failure in the reflow soldering process of a hard disk drive factory was found resulting in defective products; therefore, a solution to resolve this problem must be researched. This article reports a solution to the aforementioned problem by using transient thermal-electric simulation to investigate the heat transfer in the welding tip and a simple experiment to verify the simulation. By using ANSYS, the simulation results revealed the temperature of welding tip. The maximum temperature was 406°C on the head tip at t=0.7s and then it rapidly decreased. The reflow soldering process failure occurred when footprint was done after 0.7s causing the temperature to be too low for melting the solder so the arm and HGA were unable to connect to each other. We proposed simple solutions and ways to improve the efficacy of the reflow soldering process; e.g., footprints should be done at 0.7s, and the welding tip's material should be changed from haynes 230 to 556. After the factory implemented our results, the problem could truly be resolved. Not only do products have a higher quality but also miscellaneous expenses from defective products are saved.

1. Introduction

A hard disk drive (HDD) is computer data storage equipment. In 2015, over 469 million HDD units were exported worldwide with an overall value of 28,140 million USDs. Over 60% of HDDs traded in the global market are manufactured in Thailand. Therefore, Thailand may be deemed as the World's center of HDD manufacturing. The HDD consists of over 2,000 electronic parts, all of which must be manufactured in a clean room by advanced manufacturing technology. The arm and head gimbal assembly (HGA) are important parts of the HDD used for supporting read/write head's stability to record data on platter correctly. In the HDD manufacturing process, the HGA was connected to the arm using reflow soldering process by the welding automation machine (WAM). The reflow soldering process may be explained as follows: a target of connection between the arm and HGA is called the connected area, which exists both on the arm and on the HGA. The connected area of the arm will already have a small drop of specific lead. When the connected area of both the HGA and arm are aligned, the WAM's control system will press the welding tip down, leaving a footprint on the connected area at a temperature of approximately 400°C. The special type of lead will melt and connect the arm and HGA together. The reflow soldering process uses 2.5 s to complete in a cycle time. Figure 1 shows the connected area, HGA, and arm inside a completed HDD. In a conceptual design of the welding tip based on Joule heating effect, heat with high temperature will be generated at the head tip by applying suitable alternating current or voltage at tail tip. To control a cycle time and the maximum temperature generated at the head tip to make reflow soldering process precisely, the WAM has an automated system designed for supporting this purpose.

This research is collaboration with an HDD manufacturing factory. During the past, research and development of the reflow soldering process had been carried out using methods of trial and error for over a decade. This method

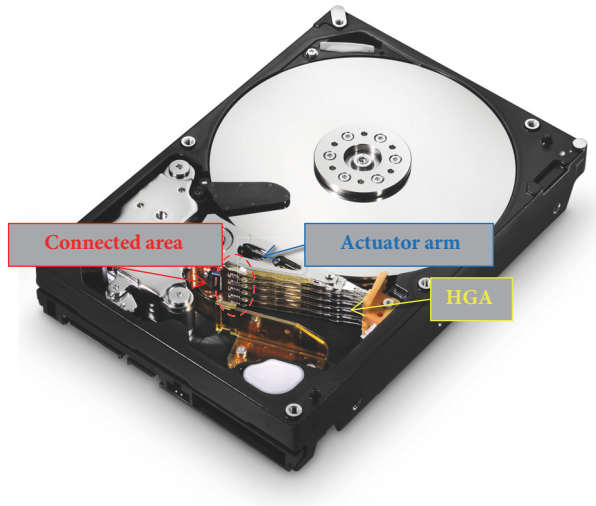

Figure 1: Connected area, HGA, and arm of HDD.

costed the factory excessive expenses in experimenting to find a suitable welding tip. Worse, the development of welding tip once used in the manufacturing process was not problem-free. Sometimes the lead did not melt, making it impossible to connect the HGA and arm resulting in defects which must be eliminated. This waste costed several million USD in loss per year. The factory anticipated that the problem rooted from unsuitable heat transfer in the welding tip; therefore, an urgent attempt to solve this problem must be undergone. The factory consulted the authors. The authors accepted and responded by using transient thermal-electric analysis, computer simulation, and suitable experiment to solve the problem. Moreover, the experiment for validation would be set up using instruments readily available in the factory so the factory's engineers might apply our methodology for own further research.

In searching articles related to thermal-electric analysis, we found that most researches focus on using thermal-electric analysis to study, design, build, or improve thermoelectric generators (TEGs) that have high efficacy in converting heat energy to electric energy, since it is environment-friendly [1–3]. Computer simulation using the ANSYS program is an important tool to pervasively develop this research branch, e.g., to design, simulate, and optimize the TEGs for higher efficacy [4–7]. The most similar research to ours is Bumrungwong's, which used thermal-electric simulation to enhance the hot bar's heat transfer efficiency for a hard disk drive factory [8]. All mentioned simulations in the research are steady-state; therefore, the results are not ample enough to use in certain researches that require the study in time-dependent conditions and thus require transient simulation [9, 10]. The difference of this research from others which is our challenge is that this research converts alternating current to heat in a short amount of time, which steady-state simulation is not enough to resolve the problem. Time greatly affects the experiment and simulation. Therefore the methodology used with steady-state conditions from others cannot be applied to our research, requiring us to seek for other suitable methodologies that simulate and investigate the heat transfer in the welding tip to solve the factory's problem.

This article reports our methodology including thermal-electric simulation and experiment setup to investigate the heat transfer in transient mode of welding tip using actual conditions collected at the factory. Also, the cause to why the lead would not melt along to the solution to the problem will also be found. Moreover, simulation results will be analyzed to find ways to improve the efficacy in the footprint process.

2. Theoretical Background

The welding tip functions by the Joule heating effect, also known as resistive heating and Ohmic heating, or the effect of transferring electricity to the conductor, generating heat. The basic equation used to study Joule heating effect is the same used to study the thermoelectric effect, as presented in (1) and (2). Equation (1) derived from heat flow equation, while (2) derived from the continuity of charge equation [6, 11]:

$$\rho C\left(\frac{\partial T}{\partial t}\right) + \nabla \bullet ([\Pi] \bullet \boldsymbol{J}) - \nabla \bullet ([\lambda] \bullet \nabla T) = \dot{q} \tag{1}$$

$$\nabla \bullet \left([\varepsilon] \bullet \nabla \frac{\partial \varphi}{\partial t}\right) + \nabla \bullet ([\sigma] \bullet [\alpha] \bullet \nabla T) + \nabla \bullet ([\sigma] \bullet \nabla \varphi) = 0. \tag{2}$$

Equations (1)-(2) are used as the fundamental information for selecting suitable materials to be invented and assembled to welding tip. Materials used to make the welding tip should be alloy with low resistivity and low specific heat but high thermal conduction. Materials found to be suitable for making the welding tip are copper alloy and haynes 230. A model of the welding tip will be explained in Section 4.1.

The finite element method for thermal-electric simulation in ANSYS, in the case that material properties relied on the temperature and time (transient), is nonlinear equation [6, 12]:

$$\begin{bmatrix} C^{TT} & 0 \\ 0 & C^{\varphi\varphi} \end{bmatrix} \begin{Bmatrix} \dot{T}_e \\ \dot{\varphi}_e \end{Bmatrix} + \begin{bmatrix} K^{TT} & 0 \\ K^{\varphi T} & K^{\varphi\varphi} \end{bmatrix} \begin{Bmatrix} T_e \\ \varphi_e \end{Bmatrix} = \begin{Bmatrix} Q \\ I \end{Bmatrix} \tag{3}$$

Transient thermal-electric simulation to investigate the heat transfer can be achieved by solving (1)-(3). In this research, the welding tip is complicated model and has many boundary conditions. Since we require high solution accuracy, we are not able to solve all equations manually, hence requiring the thermal-electric simulation in ANSYS software. ANSYS is a popular engineering simulation program widely used to solve various problems in the industry to help simulate and solve the equation successfully.

When the welding tip is stimulated by alternating current, heat will be generated and then released to air called convection. The equation that covers convection heat transfer is defined by Newton's law of cooling:

$$\frac{q}{A} = h(t)\left(T_s - T_f\right). \tag{4}$$

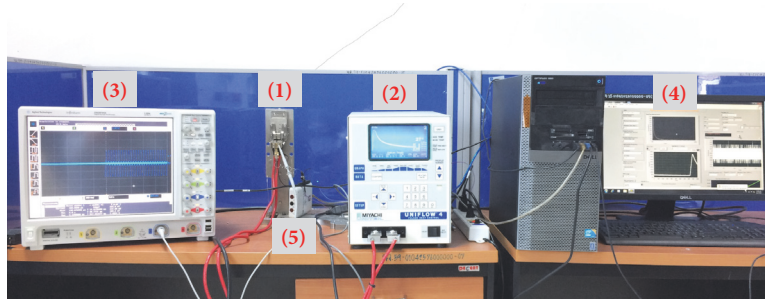

Figure 2: Instruments setup in the experiment.

$h(t)$ in (4) is the value that depends on time, which can be determined by the experiment. It is necessary for determining $h(t)$ to set in the boundary conditions. A high value of $h(t)$ indicates that an object rapidly loses heat to the surrounding air before cooling down.

3. Experiment

In this section, we explain the experimental setting, which is a novel experiment. No researches have set the experiment to measure the temperature of welding tip like this before. All boundary conditions are set to be similar to practical use in the reflow soldering process of the factory as possible. The data collected from this experiment is necessary for setting the boundary conditions in ANSYS to be explained later in Section 4.3. Some results will be used for validation. Figure 2 presents instruments used in the experiment consisting of (1) the welding tip, (2) Uniflow#4, (3) digital oscilloscope, (4) computer with LabVIEW program, and (5) data acquisition (DAQ) box. The welding tip was installed on a stand. Model and details of the welding tip will be mentioned in Section 4.1. Uniflow#4 applied alternating current to the welding tip. We can control a characteristic of alternating current by adjusting voltage and applied time by Uniflow#4. A digital oscilloscope was employed to measure the real applied voltage and frequency at the tail tip. We found that the results recorded from the oscilloscope can be plotted into a sine curve in terms of $V(t) = 1.66 \sin [2\pi(50)t]$. The total time of applied alternating current was 0.7s. During 0.615-0.7s the maximum voltage declined 17% per period from the previous point. The computer with LabVIEW program was connected to the DAQ box. The DAQ box was connected to the thermocouple with $\pm 0.01^{\circ}$C accuracy to measure temperature at the measured point. The LabVIEW program was written to control precision of time, which was every 5 ms per point. In fact, ANSYS thermal-electric simulation for this boundary condition can be used in the case that problems found are steady-state only. Still, we were able to do transient calculations since we wrote special commands in ANSYS Parametric Design Language (APDL) to constrain each element to be calculated in transient mode. This is a special technique which the author thinks is beneficial towards readers who would like to research in this field. That command may be written as "ANYTYE, TRANS".

In measuring the temperature, we chose the measured point to be slightly away from the head tip, similar to the actual setting at the factory, since the head tip was used in making the footprint onto the connected area in the welding process, thus making it impossible to measure the temperature at the point. For convenience purposes, the factory assumed that the temperature at the measured point and head tip is equal. Afterwards, the temperature from the measured point was used as reference for an automation system to control the footprint process. Since the welding process took a cycle time of 2.5 s, the computer would record the temperature versus time for all 500 measured points. We expected that this is detailed enough to validate all results from the simulation.

4. Simulation

4.1. Welding Tip. Figure 3 shows a simplified solid model of welding tip. This type of welding tip is used for manufacturing 3.5-inch hard disk drive. A small picture presents the actual welding tip near the measured point. Below, there are two signal wires: first wire was connected to the thermocouple and the DAQ box to measure the temperature versus time. Another wire was connected to the Uniflow#4 and the WAM for feedback control system. Above, signal wires were connected to the digital oscilloscope for measuring the applied voltage from Uniflow#4. The welding tip consists of 3 materials: copper alloy, stainless steel, and haynes 230. The copper alloy is divided into 2 bars separated from one another where alternating current applied through both sides. Haynes 230 was between the two bars of copper alloy. It was designed based on the Joule heating principle to generate high temperature at the head tip once applied with alternating current. Haynes 230 is a key material following the conceptual design since its property is excellent in high temperature and has long-term thermal stability and outstanding resistance to oxidizing environment. Lastly, nut and bolt were made of stainless steel, which fixed the copper alloy and haynes 230 together.

4.2. Mesh Model. Figure 4 shows the mesh model, all of which is hexahedral mesh with 29,138 elements and 110,572 nodes. The head tip has the smallest element with 0.1 mm in sizing. The copper alloy bars have the largest element with 1 mm in

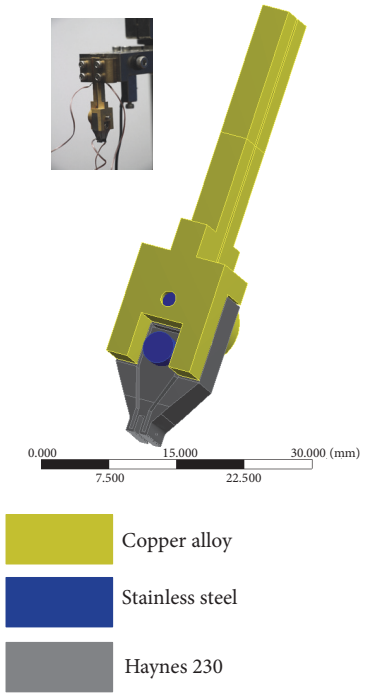

Figure 3: A simplified solid model of welding tip.

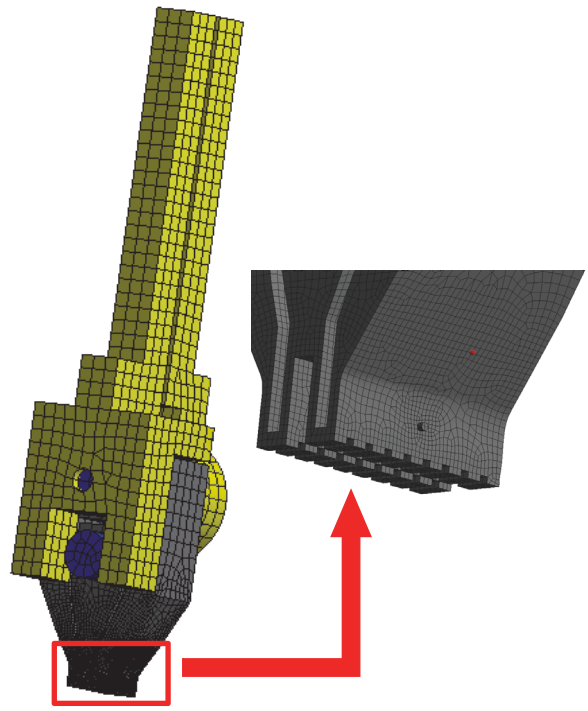

Figure 4: Mesh model of welding tip.

sizing. This mesh type provides the most accurate solution using the least amount of computational time.

4.3. Boundary Conditions. Figure 5 shows the boundary conditions setting in the transient thermal-electric simulation of ANSYS. One side of the tail tip of copper alloy was set using $V(0) = 0$ and $T(0) = 30^{\circ}\text{C}$ which was at room temperature. The other tail tip was $V(t) = 1.66 \sin [2\pi(50)t]$ and changed according to the data measured from the digital oscilloscope as mentioned in Section 3.

The *h(t)* value is vital in determining boundary conditions, which depend on both time and temperature. The more intense the heat and shorter the time, the higher the *h(t)* value. From studies, no *h(t)* values fit with the welding tip shape and operating conditions in our research. This is the challenge and difficulty in our work. We must seek the value by calculating along with experimenting. In order to find a suitable *h(t)* value in our work, we experimented to observe the heat transfer behavior at several welding tips used at the factory along with studying additional and related documents with thermal-electric devices and materials [8, 13]. We realize that when copper alloy and stainless steel receive electric currents, the temperature does not rise to be too intense and change slowly when compared to haynes 230, where temperature rises quickly. Thus, for simulation convenience we set the properties of copper alloy and stainless steel, e.g., specific heat, thermal conduction, resistivity to be constant values, and not altering to the time and temperature. If the material properties that we set are not too different from the actual values and ANSYS program calculates and discovers an unreasonable value, the program's solver with an inner

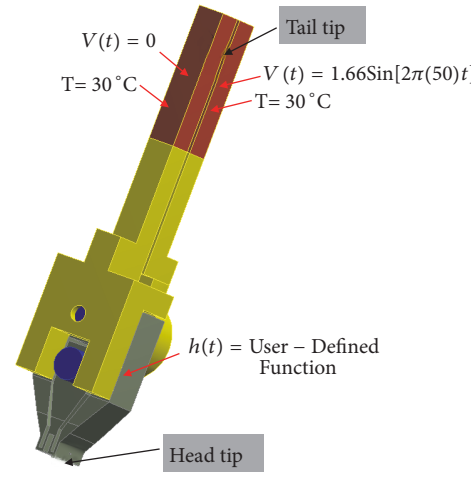

Figure 5: The boundary conditions setting in ANSYS.

function will compensate values to be more realistic [12]. As for haynes 230, material properties depend on the time and temperature. For the *h(t)* value calculation for haynes 230, we wrote a User-Defined Function (UDF) program to calculate the *h(t)* value at an amount great enough to accurately check occurring heat transfer. In this procedure, we used 500 values to compile with the amount of time steps in the analysis setting. Heat flux *q/A* from (4) can be found using the function probe in ANSYS at the measured point. As for T_s and T_f, they were gained from actual experiment using a thermocouple accordingly. This UDF will

Table 1: Material properties of copper alloy.

Properties (Unit)/ Temperature (°C)	Specific heat (J/kg-°C)	Thermal conductivity (W/m- °C)	Isotropic resistivity (Ω-m)	Convection film coefficient (W/m^2-K)
25	385	401	1.69E-08	35
100	385	398	2.28E-08	35
Density			8,300 kg/m^3	

Table 2: Material properties of stainless steel.

Properties (Unit)/ Temperature (°C)	Specific heat (J/kg-°C)	Thermal conductivity (W/m- °C)	Isotropic resistivity (Ω-m)	Convection film coefficient (W/m^2-K)
25	480	15.1	7.70E-07	35
Density			7,750 kg/m^3	

Table 3: Material properties of haynes 230.

Properties (Unit)/ Temperature (°C)	Specific heat (J/kg-°C)	Thermal conductivity (W/m- °C)	Isotropic resistivity (Ω-m)	Convection film coefficient (W/m^2-K)
25	397	8.9	1.250E-06	1.8E12
100	419	10.4	1.258E-06	8.8E11
200	435	12.4	1.265E-06	4.5E11
300	448	14.4	1.273E-06	3.0E11
400	465	16.4	1.284E-06	1.8E11
Density			8,970 kg/m^3	

be inputted into ANSYS to simulate occurring heat transfer. The more detailed and numerous *h(t)* is, the more accurate the simulation results. Tables 1–3 show some of the necessary material properties of copper alloy, stainless steel, and haynes 230, as to determine boundary conditions. All values were provided by the vendors, except for the *h(t)* of haynes 230, which the researchers calculated. We cannot present all 500 *h(t)* values of haynes 230 into this article, since it will make the document too long. Naturally, the true properties of the *h(t)* value depend on the airflow, temperature, and welding tip shape during convection. Thus, the material properties in Tables 1–3 are an average value for primary simulation only. The interesting point from this research is that the *h(t)* in Table 3 is an important value we calculated from transient state experimenting for every 5ms per point which is extremely high as it depends on the time and temperature while convection occurred. But the *h(t)* value of objects in general research is low due to being calculated from a steady-state condition at a low temperature. When the *h(t)* is high, the welding tip emits heat quickly. If *h(t)* in a steady state is used, the simulation will be wrong. We also learned that if the welding tip shape and size are changed, the *h(t)* value also varies accordingly. Therefore, to check the heat transfer occurring at the welding tip, coupling both simulation and experiment is necessary for accurate results.

In analysis setting, the calculation was divided into 500 steps, 5 ms per step. Each step has 20 iterations per step; therefore, the computer must calculate all 10,000 iterations covering 2.5 s of cycle time for footprint process. This calculation was deemed as highly detailed. From all these settings, we believed that the simulation provided credible and accurate results.

5. Results and Discussion

By using the transient thermal-electric simulation in ANSYS to investigate the heat transfer and determine the temperature in the welding tip, Figure 6 reveals the temperature comparison results from the simulation and experiment at the measured point. We found that they were very well consistent. The maximum discrepancy was 2.89% at t=0.795s, in which T_{exp} = 390.4°C and T_{sim} = 379.1°C. This might be due to the fact that we used 5 ms per time step in calculation. At t = 0.7 to 1.5s, the welding tip released heat rapidly. If we used 1 ms for time step and the material properties in Tables 1–3 that depend on the time and temperature are more detailed**,** it was assured that the discrepancy would no longer be presented but that action requires more computational time. Moreover, we also observed that the temperature at the nut, bolt, and tail tip was around 30-40°C throughout for both simulation and experimental results. All these make us confident that our simulation and experimental results are deemed accurate and reliable.

To simulate the transient thermal-electric heat transfer, Figure 7 shows the temperature distribution during 0–2.5s. Notice the start at t=0s until near t =0.7s. The welding tip quickly heated up from the tail to the head. At t= 0.7s, the head tip's maximum temperature was 406°C before gradually cooling down. The behavior of changing in temperature versus time is consistent with the experimental results reported

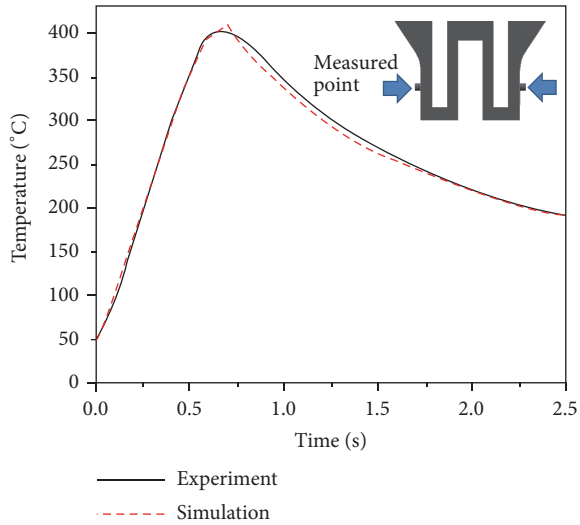

Figure 6: Temperature comparison results from the simulation and experiment at the measured point.

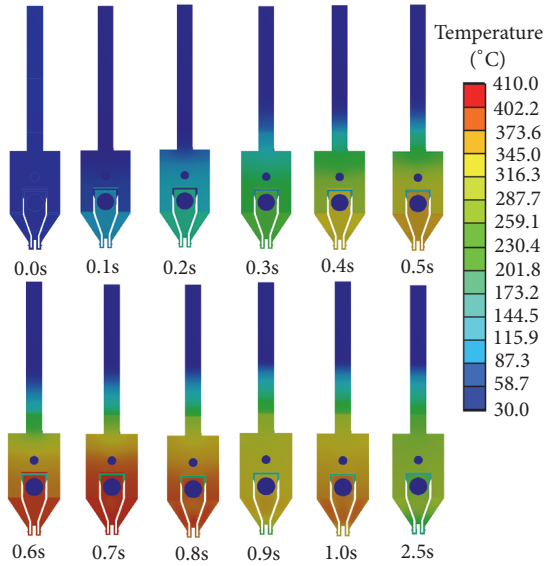

Figure 7: Temperature distribution on welding tip surface during 0–2.5s.

in Figure 6. Haynes 230 has higher temperature than other materials, especially at the head tip. Therefore, the welding tip could be designed to have the highest temperature at the head tip as precise as the conceptual design. Figure 8 shows the highest temperature at the head tip specifically for 0.5-1.0s. From 0.7s to 1.0s, the maximum temperature promptly lessened 100°C within a short amount of time. This figure also indicated that, in using the welding tip, footprints should be done at 0.7s for the highest efficacy in heat generating.

Because in real reflow soldering process, the factory measured the temperature at the measured point rather than the inconvenient head tip that was used in making the footprint. The temperature collected from the measured point was sent to a feedback control system of the WAM as temperature reference. The WAM has functioned continuously, which assumed that the temperatures at head tip and at measured point were equal for convenience purposes. Due to this, we also calculated the temperature at head tip and measured point. Compared results are shown in Figure 9. It was found that the temperatures were similar to each other only during the first 0-0.7s. After 0.7s onwards, after the highest temperature, when the time was increased, the temperature even showed greater differences. At t=2.5s, temperature differed at about 10%. All this may be used to explain the reason why sometimes while making footprints, the lead melts and sometimes it did not. This is due to the fact that the lead is a special type that has a melting point about 400°C. Thus, when the lead did not melt it is because the machine was too slow to make the footprint and the temperature at the head tip below 400°C already. For example, if the footprint was done at t=0.75s, the temperature at the head tip was 390°C and measured point was 401°C. To solve this problem, the engineers should design a controlled footprint processing system that makes footprint at precisely 0.7s. At this time, the temperatures of head tip and measured point were 406°C. This way the lead will melt resulting in no product defects.

To enhance the efficacy of the welding tip, haynes 214, 242, and 556 were chosen to simulate the heat transfer and temperature. The reason why these 3 were selected is due to their tensile strength which is equal to or greater than haynes 230 of the original welding tip. All haynes' properties were given by the vendors. Figure 10 reports the temperature at head tip for all types of haynes. We found that the temperatures of all types were similar to each other in the first 0.7s of cycle time. At t= 0.7s, haynes 556's maximum temperature was slightly higher than others by 5°C. Afterwards, haynes 556 is the slowest type to release heat. This may be applicable in controlling Uniflow#4. When the first footprint is completed, the engineers will design Uniflow#4 to apply less voltage. Due to the lesser amount of time, the temperature will rise to its highest faster than haynes 230. This can be considered as energy conservation. Moreover, haynes 556 is also durable towards reshaping and can absorb more impact force; therefore, it is suitable to develop to be more effective welding tip.

In actual manufacturing, the welding tip was installed into the WAM inside the clean room with cool air supplied as reported in the works of Thongsri et al. [14–16] Within the machine, there was a laminar flow generated by fan filter units to ventilate the air in and out the WAM with temperature lower than 24.5°C. This environment could slightly affect the welding tip lose heat faster rate. Hence, if the further research included thermal-electric simulation and computational fluid dynamics within the laminar flow of a machine is conducted, research results will be even more accurate and beneficial.

The results of this research were submitted to the HDD factory. The changes in footprint process following our recommendation reduced the factory's costs in 2 ways; 1st is development in the laboratory. A newly designed welding tip: in the past procedures were the trial and error method which the factory must order large quantities of

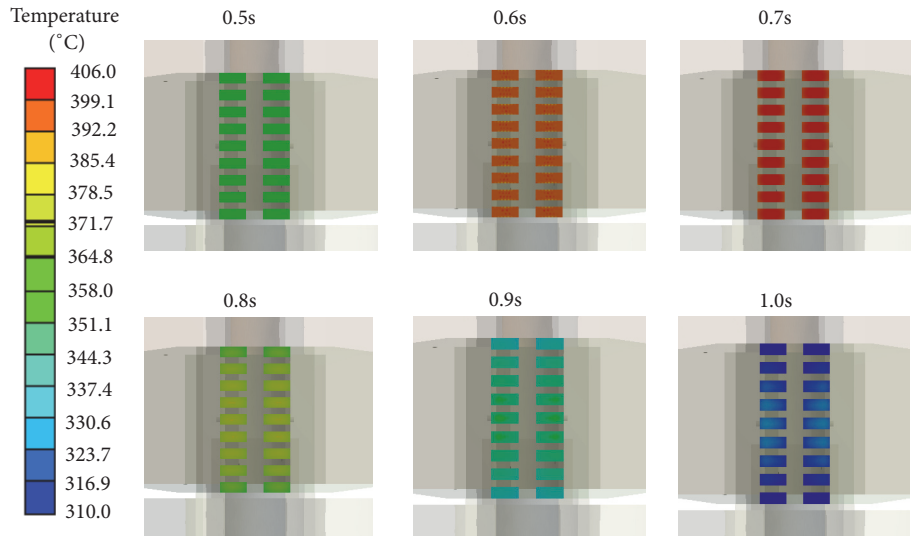

Figure 8: The highest temperature at head tip during 0.5–1.0s.

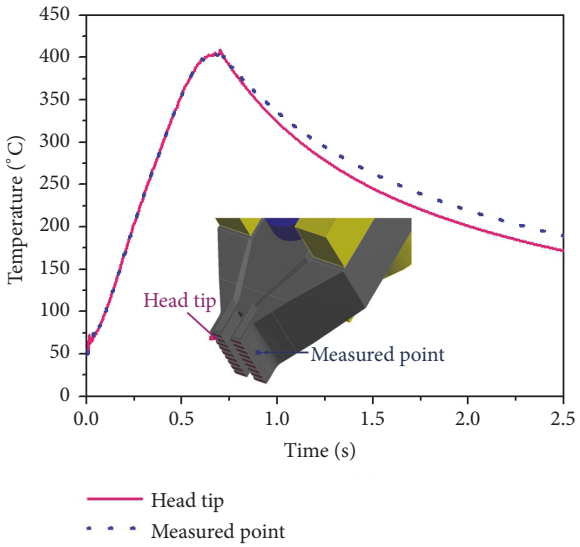

Figure 9: Temperature comparison results from the head tip and the measured point.

welding tip prototypes to experiment and find the best operating condition. Once the tips have deteriorated, they will be disposed of immediately. After applying research results, factory engineers can design highly efficient welding tips as demanded. This reduces the ordered welding tip prototypes for trial by 50%. Moreover, after experimenting the welding tips can still be used. As for the 2nd way in actual usage, the welding tip had greater efficiency, durability, and an extended usage life, reduced the quantity of defective products of 15,000 pieces per year, enhanced product quality, and saved more than 0.15 million USD annually.

6. Conclusion

This article is an author's experience in solving the problem found at the HDD manufacturing process. Welding tips are used as the equipment in making footprint to connect the arm and HGA together by using a specific lead as solder in the reflow soldering process. Applying alternating current to the welding tip, heat with high temperature is generated at the head of welding tip based on Joule heating principle.

In making footprints, the head tip is pressed onto the lead to melt in order to connect the arm and HGA parts together. Previously, reflow soldering process error was in certain products when the lead did not melt. This resulted in unconnected arms and HGAs, causing losses towards the factory. A solution must be found urgently. We used transient thermal-electric simulation in the ANSYS program to simulate heat transfer that happens within 2.5s of cycle time by using the actual boundary conditions collected from the factory. The simulation results were confirmed by the novel experiment that we set up using simple instruments readily available at the factory. The simulation results showed the temperature in all areas of the welding tip. At the start of the process, the temperature increased rapidly with a maximum at t=0.7. The maximum temperature was 406°C at the head tip, and then it slowly declined. At t=2.5s, the temperature of the head tip decreased to 170°C. Welding process failure might be caused by making footprints after 0.7s. After this time, the temperature of the head tip would drop to lower than 400°C, which could not melt the lead and thus failing to connect the arm and HGA together. In order to solve this problem, we recommended the factory's engineers that footprints should be precisely done at t=0.7s.

From the simulation, we also found that when the welding tip material was changed from the traditional model using haynes 230 to haynes 556, the maximum temperature at head tip increased 5°C higher along with a slower heat-release rate. Other than this, haynes 556 also has yield tensile strength

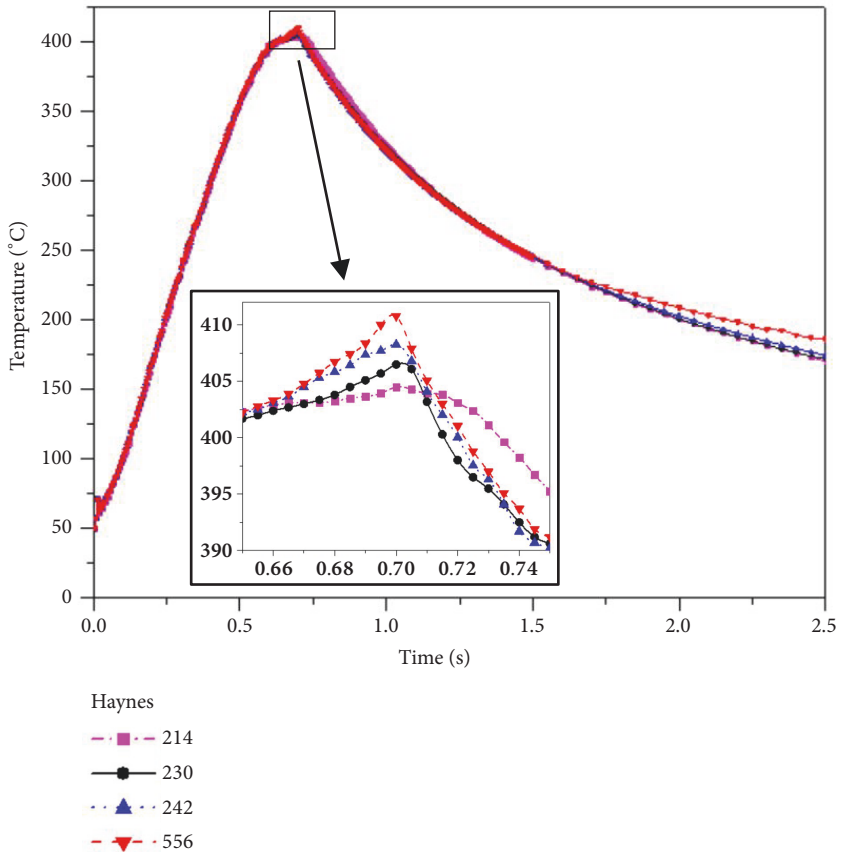

Figure 10: Simulated temperatures at the head tip for haynes 214, 230, 242, and 556.

that is greater than haynes 230 as well, making it suitable to develop into highly-efficient welding tips in the future. The results of this research, once applied to the factory, helped the factory save costs more than 0.15 million USD annually.

Nomenclature and Abbreviations

T: Absolute temperature (K)
T_f: Air temperature (K)
A: Area of surface according to the heat flux (m^2)
h: Convection film coefficient (W/m^2-K)
ρ: Density (kg/m^3)
$[C^{\varphi\varphi}]$: Dielectric damping matrix
$[\varepsilon]$: Dielectric permittivity matrix (F/m)
$[\sigma]$: Electric conductivity matrix (S/m)
$\boldsymbol{J}$: Electric current density (A/m^2)
$\{I\}$: Electric power load vector
φ: Electric scalar potential (V)
$[K^{\varphi\varphi}]$: Electric stiffness matrix
HDD: Hard disk drive
HGA: Head gimbal assemble
q: Heat generation (W)
$\dot{q}$: Heat generation rate per unit volume (W/m^3)
$[\Pi]$: Peltier coefficient matrix (V)
$[\alpha]$: Seebeck coefficient matrix (V/K)
$[K^{\varphi T}]$: Seebeck stiffness matrix
C: Specific heat capacity (J/kg-K)
T_s: Surface temperature (K)
$[\lambda]$: Thermal conductivity matrix (W/m-K)
$[C^{TT}]$: Thermal damping matrix
$[K^{TT}]$: Thermal stiffness matrix
t: Time (s)
$\{Q\}$: Vector of combined heat generation (W/m^3)
$\{\varphi_e\}$: Vector of nodal electric potential
$\{\dot{\varphi}_e\}$: Velocity vector of nodal electric potential
$\{T_e\}$: Vector of nodal temperature
$\{\dot{T}_e\}$: Velocity vector of nodal temperature
$V(t)$: Voltage applied by Uniflow#4 (V)
WAM: Welding automation machine.

Data Availability

The data used to support the findings of this study are available from the corresponding author upon request.

Conflicts of Interest

The author declares that there are no conflicts of interest for this article.

Acknowledgments

This research was supported by College of Advanced Manufacturing Innovation, King Mongkut's Institute of Technology Ladkrabang.

References

[1] D. Champier, "Thermoelectric generators: A review of applications," *Energy Conversion and Management*, vol. 140, pp. 167–181, 2017.

[2] W. He, G. Zhang, X. Zhang, J. Ji, G. Li, and X. Zhao, "Recent development and application of thermoelectric generator and cooler," *Applied Energy*, vol. 143, pp. 1–25, 2015.

[3] D. Zhao and G. Tan, "A review of thermoelectric cooling: materials, modeling and applications," *Applied Thermal Engineering*, vol. 66, no. 1-2, pp. 15–24, 2014.

[4] A. S. Korotkov, V. V. Loboda, S. B. Makarov, and A. Feldhoff, "Modeling thermoelectric generators using the ANSYS software platform: Methodology, practical applications, and prospects," *Russian Microelectronics*, vol. 46, no. 2, pp. 131–138, 2017.

[5] M. N. Zulkifli, I. Ilias, A. Abas, and W. M. W. Muhamad, "Finite element analysis of thermoelectric generator with aluminum plate for waste heat recovery application," *International Journal on Advanced Science, Engineering and Information Technology*, vol. 7, no. 4, pp. 1328–1333, 2017.

[6] E. E. Antonova and D. C. Looman, "Finite elements for thermoelectric device analysis in ANSYS," in *Proceedings of the 24th International Conference on Thermoelectrics (ICT '05)*, pp. 19–23, IEEE, Piscataway, NJ, USA, June 2005.

[7] Y. Shi, X. Chen, Y. Deng et al., "Design and performance of compact thermoelectric generators based on the extended three-dimensional thermal contact interface," *Energy Conversion and Management*, vol. 106, pp. 110–117, 2015.

[8] J. Bumrungwong, "The Study of the hot bar for reflow process in interconnecting of head stack assembly," *International Journal of Applied Computer Technology and Information System*, vol. 4, no. 2, pp. 10–13, 2015.

[9] W. Li, M. C. Paul, A. Montecucco et al., "Multiphysics simulations of thermoelectric generator modules with cold and hot blocks and effects of some factors," *Case Studies in Thermal Engineering*, vol. 10, pp. 63–72, 2017.

[10] W. Li, M. C. Paul, A. Montecucco et al., "Multiphysics Simulations of a Thermoelectric Generator," *Energy Procedia*, vol. 75, pp. 633–638, 2015.

[11] L. D. Landau, E. M. Lifshitz, and L. P. Pitaevskii, *Electrodynamics of Continuous Media*, Butterworth-Heinemann, Oxford, UK, 2nd edition, 1984.

[12] Ansys, *Inc Nonlinear and transient thermal analysis, Ansys Mechanical Heat Transfer*, 2016.

[13] S. K. Thangaraju and K. M. Munisamy, "Electrical and Joule heating relationship investigating using finite element method," in *IOP Conference Series: Materials Science and Engineering*, vol. 88, 2015.

[14] J. Thongsri, "A successful CFD-based solution to a water condensation problem in a hard disk drive factory," *IEEE Access*, vol. 5, pp. 10795–10804, 2017.

[15] J. Thongsri, "A Problem of Particulate Contamination in an Automated Assembly Machine Successfully Solved by CFD and Simple Experiments," *Mathematical Problems in Engineering*, vol. 2017, Article ID 6859852, p. 9, 2017.

[16] J. Thongsri and M. Pimsarn, "Optimum airflow to reduce particle contamination inside welding automation machine of hard disk drive production line," *International Journal of Precision Engineering and Manufacturing*, vol. 16, no. 3, pp. 509–515, 2015.